



[http://revistas.unipamplona.edu.co/ojs\\_viceinves/index.php/BISTUA](http://revistas.unipamplona.edu.co/ojs_viceinves/index.php/BISTUA)

## A facile microwave-assisted synthesis of ZnO nanoparticles and their photocatalytic activity: Effect of pH

### Síntesis asistida por microondas de nanopartículas de ZnO y su actividad fotocatalítica: Efecto del pH

Aura S. Merlano; Ángel Salazar

Grupo de Óptica y Espectroscopía (GOE), Centro de Ciencia Básica, Universidad Pontificia Bolivariana, Medellín, Colombia

Contacto: [aura.merlano@upb.edu.co](mailto:aura.merlano@upb.edu.co)

Recibido: Noviembre 25, 2020. Aceptado: Diciembre 22, 2020

<https://doi.org/10.24054/01204211.v2.n2.2020.4436>

#### Resumen

Este estudio reporta una síntesis fácil, libre de surfactantes y asistida por microondas para la producción de nanopartículas de óxido de zinc (ZnO). Se investigó el efecto del valor del pH sobre las propiedades químicas, ópticas, morfológicas y fotocatalíticas de las nanopartículas de ZnO. Las nanopartículas se caracterizaron mediante microscopía electrónica de barrido (SEM), espectroscopía infrarroja por transformada de Fourier (FTIR), espectroscopía de rayos X por dispersión de energía (EDS) y espectroscopía UV-visible (UV-Vis). El análisis SEM muestra que el tamaño de las partículas disminuye con el aumento del valor de pH. Los espectros UV-Vis muestran picos de absorción excitónica alrededor de 334-359 nm. Se encontró que la brecha de energía de las muestras disminuye con el aumento del valor de pH. Finalmente, se evaluó la eficiencia fotocatalítica de los nanomateriales de ZnO mediante la degradación de naranja de metileno (MO) bajo irradiación de luz UV-A y se logró una eficiencia de degradación del colorante del 93.04% para la muestra de ZnO con pH-13. Los resultados experimentales confirman que la ruta propuesta para producir ZnO es fácil, reproducible y amigable con el medio ambiente. Además, el nano ZnO tiene un gran potencial como fotocatalizador para eliminar compuestos orgánicos.

**Palabras clave:** ZnO; Fotocatálisis; Síntesis asistida por Microondas; pH.

#### Abstract

This study reports an easy, surfactant-free and microwave-assisted synthesis for the production of zinc oxide (ZnO) nanoparticles. The effect of pH value on chemical, optical, morphological and photocatalytic properties of ZnO nanoparticles were investigated. The nanoparticles were characterized using scanning electronic microscopy (SEM), Fourier transform infrared spectroscopy (FTIR), energy dispersive X-ray spectroscopy (EDS) and UV-visible spectroscopy (UV-Vis). SEM analysis shows that the particle size decreases with increase in pH value. The UV-Vis spectra show excitonic absorption peaks around 334-359 nm. It was found that the energy gap of the samples decreases with the increase in pH value. Finally, the photocatalytic efficiency of ZnO nanomaterials were evaluated by degradation of methylene orange (MO) under UV-A light irradiation and 93.04% degradation efficiency of the dye was achieved for ZnO sample with pH-13. The experimental results confirm that the proposed route to produce ZnO is easy, reproducible and friendly with the environment. In addition, the nano ZnO has great potential as a photocatalyst for removing organic compounds.

**Keywords:** ZnO; Photocatalysis; Microwave assisted synthesis; pH.

## 1 Introduction

In recent years, zinc oxide (ZnO) nanomaterials have acquired great interest in the scientific community due to its physico-chemical properties and low-cost production [1]. ZnO nanomaterials have potential applications in the drug-delivery [2], water purification [3], biomedical [4][5], cosmetic [6], painting [7], coatings [8] and solar cell [9] sectors. Particularly, ZnO is a powerful tool for environmental applications, due it is an efficient and synergic photocatalyst for the degradation and demineralization of various toxic organic pollutants using UV, visible or solar radiations [10-12]. In Fig. 1 a keyword co-occurrence map using the VOSViewer software is presented. The analysis of the use of ZnO nanoparticles as a photocatalyst showed that the main application is the degradation of dyes such as methylene blue, rhodamine b, methylene orange and red congo by visible and solar light. Its use is also observed in self-cleaning, water splitting and antibacterial. It can be observed that the most reported methods to obtain ZnO

nanoparticles are the hydrothermal method, sol-gel, green synthesis and electrospinning. Besides, the most reported morphologies of ZnO are nanorods, nanoparticles and core-shell. There is a wide variety of synthesis methods to produce ZnO nanostructures, but the most commonly used methods are: co-precipitation with calcination [13-14], sol-gel method with calcination [15-17], mechanical synthesis with high-energy milling [18], hydrothermal synthesis [19] and solvothermal synthesis [20-21]. However, the synthesis of nanomaterials is currently in a new stage of development, where the understanding of the synthesis mechanism and the use of environmentally friendly "green" syntheses are mandatory criteria when choosing a synthesis method [22]. In this sense, one of the most promising approaches for obtaining ZnO is the microwave-assisted synthesis [23-25]. The interest that this technique is acquiring to obtain ZnO nanostructures is reflected in the number of publications that involve the words "microwave synthesis zinc oxide nanomaterials" in the last 10 years (Fig. 2). In 2020, microwave synthesis represents 24.42% of all synthesis methods to

obtain ZnO from articles published in ScienceDirect. Furthermore, from the synthesis method, the parameters such as the concentration of the precursors, the reaction temperature, the use of surfactants, the pH value of the solution and the solvent used play a key role in the physico-chemical properties of ZnO nanoparticles. Although many studies have examined the effect of pH on the synthesis of ZnO nanoparticles and their properties (Table 1), it has not been reported yet the effect of the pH particularly in a microwave-assisted method and its influence on photocatalytic performance. In this context, we report a simple microwave-assisted synthesis of ZnO nanoparticles, and the effect of pH value on their chemical, optical, morphological and photocatalytic properties.

## 2 Materials and Methodology

### 2.1 Materials

Zinc acetate dihydrate, sodium hydroxide, ethanol and methylene orange (MO) were purchased from Sigma - Aldrich. All chemicals used in the experiments were analytical reagent grade and used as received. The aqueous solutions were prepared using ultrapure water.

**Table 1.** Investigations about the effect of pH in the ZnO synthesis method.

Method	Type of property analyzed	pH	Ref
Sol-gel	Crystallite size, particle size	6, 7, 8, 9, 10, 11	[18]
Sol-gel	Optical properties		
Sol-gel	Structural and optical properties	3, 6, 9	[19]
Sol-gel	Structural and optical properties	2, 7, 10	[20]
Sol-gel	Porosity, structural and optical properties	8, 9, 10, 11, 12	[21]
Chemical precipitation	Crystal size and photoluminescence properties	6, 8, 12, 13	[11]
Chemical bath deposition	Structural, morphological, optical and luminescence properties	5, 6, 8, 12	[22]
Chemical precipitation	Morphological properties	6, 7, 8, 9, 10, 11, 12	[23]
Hydrothermal	Morphological properties	1.8 - 12.5	[24]
Microwave hydrothermal	Structural and optical properties	7, 10, 12	[25]
Microwave-assisted method	Chemical, optical, morphological and photocatalytic properties	7, 9, 13	This work

nanomaterials” phrases published in the 2011–2020. Source: ScienceDirect (accessed on 16/11/2020).

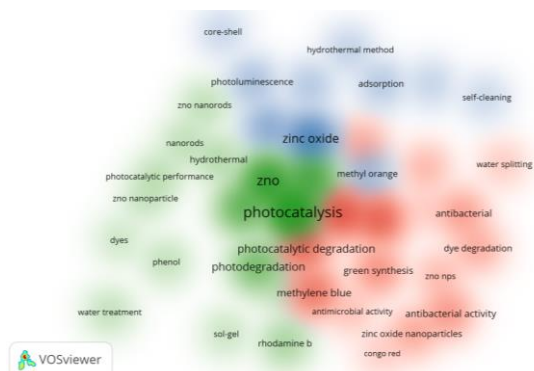


**Figure 1** Keyword co-occurrence map for “ZnO nanoparticles” AND “photocatal\*” search (time span: 2016–2020). Source: Scopus. (accessed on 01/12/2020).

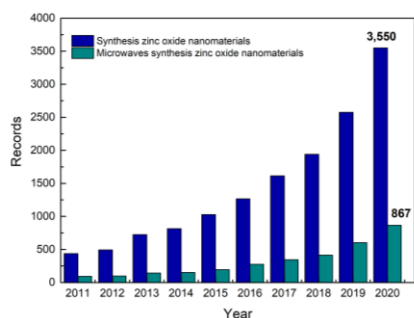


**Figure 2** The number of scientific publications referring to the search of “synthesis zinc oxide nanomaterials” and “microwave synthesis zinc oxide

### 2.2 Synthesis of ZnO nanoparticles

ZnO nanoparticles were prepared using a microwave-assisted synthesis (Fig. 3). A solution of 3 M NaOH was added to 0.02 M  $\text{Zn}(\text{CH}_3\text{COO})_2 \cdot 2\text{H}_2\text{O}$  until different pH values were obtained (7, 9 and 13). This solution was continuously stirred at 500 rpm for about 30 min. Then, the solution was transferred to a microwave oven and irradiated for 60 s. The precipitate powder was washed several times (6000 rpm/20 min) with deionized water and ethanol solution to remove impurities. Finally, the powder sample was dried at 80°C for 12 h.

### 2.3 Characterization

The morphology of the sample was analyzed using a scanning electron microscope (SEM) JEOL JSM-6490LV. Chemical group analysis of the specimen was evaluated using a Thermo Scientific Nicolet iS50 ATR-FTIR spectrometer with a wavenumber range from 400 to 4000  $\text{cm}^{-1}$ . UV-Visible spectra were recorded using a Thermo Scientific UV-Vis spectrophotometer Evolution 600.

### 2.4 Experimental procedure for photocatalytic tests

The photocatalytic activity of the ZnO nanomaterials was measured by degrading methylene orange (MO) dye under UV-A light. In a typical photocatalytic test, 10 mg of ZnO sample was ultrasonically dispersed in a 50 ml of  $8 \times 10^{-5}$  M aqueous MO solution. This solution was magnetically stirred for 60 min in dark to saturate adsorption/desorption of MO solution on the photocatalyst. Then, the dispersion was exposed to a UV lamp (365 nm, 100 W) under constant stirring. The photocatalytic degradation of MO dye was

observed by collecting aliquots of 3 mL of the dispersion each 30 min for a period of 300 min and analyzed by UV-Vis spectroscopy.

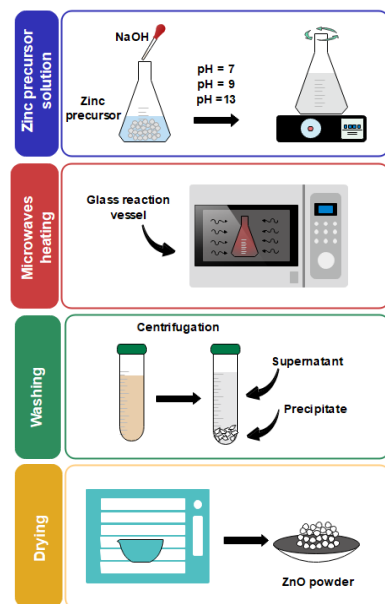


**Figure 3** Schematic representation of the microwave-assisted synthesis of ZnO nanoparticles

### 3 Results and discussion

#### 3.1 Chemical, optical, and morphological characterization

FTIR spectra of the samples synthesized in the range of 400 to 4000  $\text{cm}^{-1}$  are shown in Fig. 4. For all samples, the wide absorption bands nearby 3390  $\text{cm}^{-1}$  (stretching) and 1405  $\text{cm}^{-1}$  to 1573  $\text{cm}^{-1}$  (bending) were associated to the O–H vibrations of the water molecules adsorbed onto the samples. In addition, the absorption peak at 484  $\text{cm}^{-1}$  is corresponding to the stretching vibration of Zn–O bond. The peaks at 1966  $\text{cm}^{-1}$  to 2153  $\text{cm}^{-1}$  are assigned to the  $\text{CO}_2$  group. For pH-7 sample, other peaks at 1396, 1483 and 1567  $\text{cm}^{-1}$  were assigned to  $\text{CH}_3$  (symmetric bending) and  $\text{COO}^-$  (symmetric and asymmetric stretching) groups, respectively. Hence, during the preparation step, for this sample some residues of the acetate ion remain.

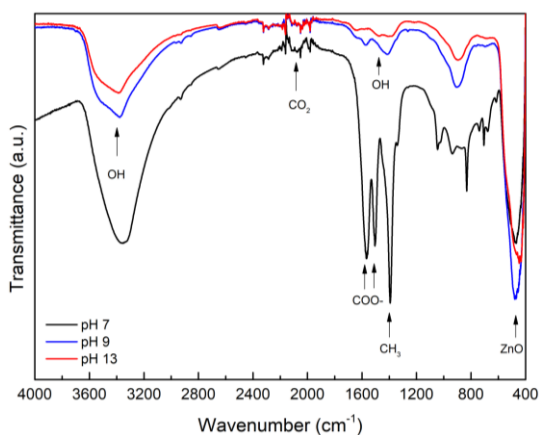


**Figure 4** FTIR spectra of ZnO nanoparticles.

The optical absorption spectra of ZnO nanoparticles were investigated in the range 300–700 nm, as shown in Fig. 5. UV-vis spectra provide the information about the excitonic and inter-band transitions of nanomaterials. The samples had an absorption peak in the UV region at 334, 352 and 359 nm for pH-7, pH-9 and pH-13, respectively. As seen, the position of the absorption peak increases gradually with the pH value. A blue shift occurred in all samples, relative to the position of the peak in bulk ZnO (approx. 388 nm). This could be attributed to a smaller crystallite size of the synthesized samples. The absence of any other band in the spectrum confirms that the synthesized product is formed only by ZnO. On the other hand, the width of the peak provides information on the dispersity of the colloidal solution. The samples with pH-9 and pH-13 present a narrow peak, which indicates a small distribution in the particle size, unlike the sample with pH-7, which presents a wider peak and therefore a greater distribution in particle size. Based on the UV-visible spectra, it was also possible to determine the band gap energy ( $E_{\text{gap}}$ ) by applying the Tauc plot method [26] (Fig. 6). According to the Tauc plot, the measures of the  $E_{\text{gap}}$  are 3.32 eV, 3.23 eV and 3.15 eV for pH-7, pH-9 and pH-13, respectively. These results are in good agreement with values reported in the literature for ZnO nanostructures synthesized by other methods [11,22].

Figs. 7–9 show the sizes and morphologies of the ZnO nanomaterials obtained by SEM. The average particle size was 307, 108 and 107 nm for pH-7, pH-9 and pH-13, respectively. It is found that the size of the particles is decreased with increasing pH value. Morphology of particles is found to be roughly spherical and oval and, no significant changes in morphology are observed with the change in pH of the solution.

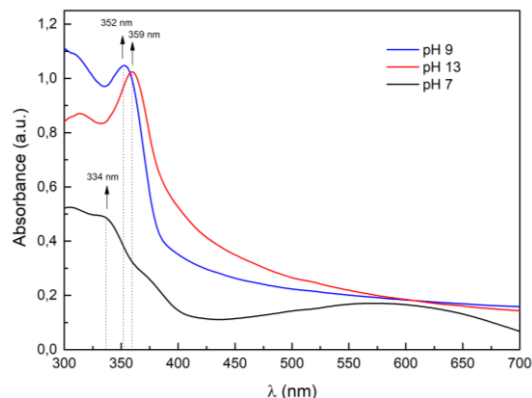


**Figure 5** UV-Vis spectra of synthesized ZnO nanomaterials.

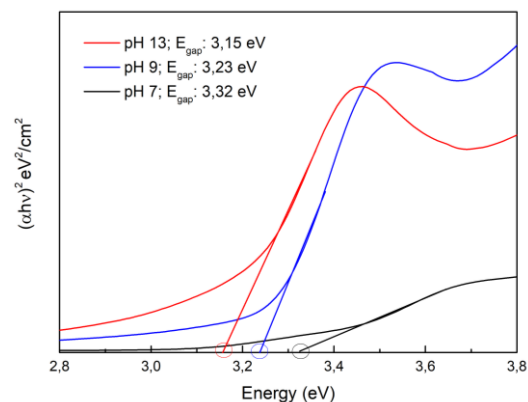


**Figure 6** Tauc plot of synthesized ZnO nanomaterials.

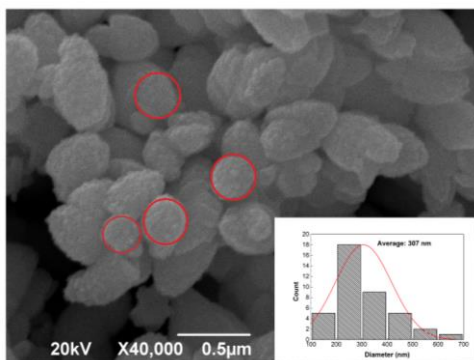


Figure. 7 SEM micrographs of ZnO-pH-7 sample.

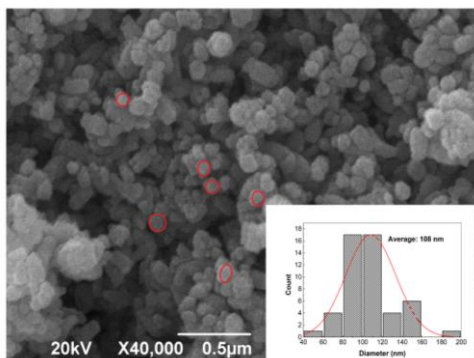


Figure. 8 SEM micrographs of ZnO-pH-9 sample.

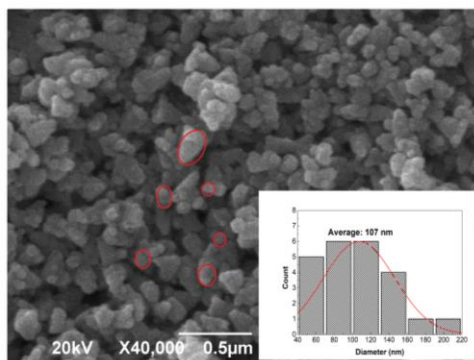


Figure. 9 SEM micrographs of ZnO-pH-13 sample.

The Energy Dispersive X-ray Spectroscopy (EDS) was used for the local determination of chemical composition of the samples. Seeing that similar spectra were recorded for all the samples, only one spectrum for pH-13 is displayed (Fig. 10). Results confirm the presence of zinc (Zn) and oxygen (O). Composition analysis of all samples is given in Table 2.

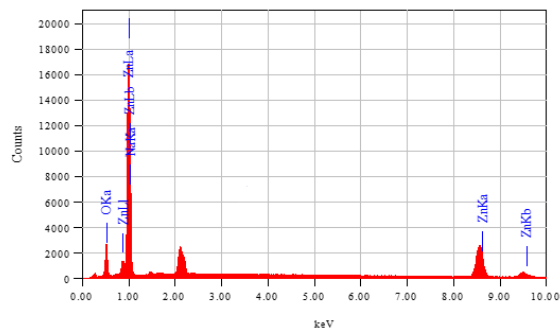


Figure. 10 EDS spectra of ZnO nanomaterials

Table 2. Chemical composition of ZnO nanomaterials

pH value	Zn (wt%)	O (wt%)	Total
7	76.82	23.18	100
9	76.41	23.59	100
13	76.84	23.16	100

### 3.2 Photocatalytic activity of ZnO nanoparticles against MO

Photocatalytic degradation of the MO dye solution was evaluated using the synthesized ZnO nanomaterials under UV-A light. Fig. 11 illustrates the normalized time-dependent photocatalytic degradation of MO solution. The degradation profile is plotted as  $C/C_0$  versus time, where  $C_0$  is the initial concentration of MO and  $C$  the concentration of MO in a particular irradiation time. The pH-7, pH-9 and pH-13 samples show a photocatalytic degradation efficiency of 42.54%, 93.04% and 59.63% after an irradiation time of 5 h, respectively. Table 3 shows in detail the percentages of adsorption, photodegradation and total removal of OM using all samples with different pH value. Fig. 12 illustrates the UV-vis absorption spectrum of the aqueous MO solution during exposure to UV-A light for different times and using ZnO-pH-9 as photocatalyst. The representative absorption peak of MO at 464 nm gradually decreases with increasing light irradiation time indicating the degradation of MO after 5 h.

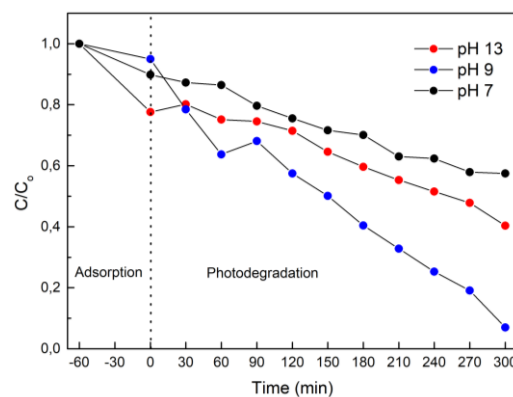


Figure. 11 Degradation efficiency (%) of MO dye at different irradiation times for ZnO nanomaterials.

Table 3. Photocatalytic performance of ZnO nanomaterials against MO

pH value	% Adsorption	%Photo-degradation	%Total removal
7	10.12	32.42	42.54
9	5.03	88.01	93.04
13	22.36	37.27	59.63

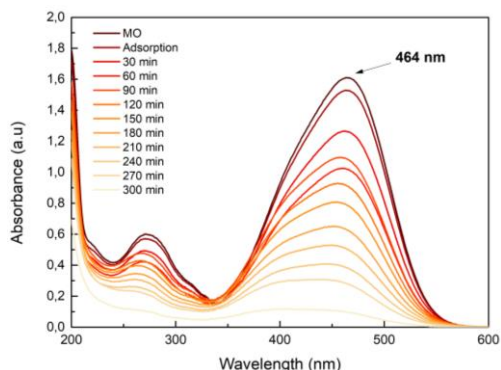


Figure 12 UV-VIS spectra of MO degradation using ZnO-pH-9.

### 3.3 Kinetic study of the photocatalytic degradation

The kinetics of dye photodegradation was estimated using all ZnO samples. The experimental data of pH-7 and pH-13 were well fitted to pseudo-first-order kinetics with a Langmuir–Hinshelwood model based on Eq. (1), where  $C_0$  and  $C$  are the initial concentration and the concentration at time  $t$  as mentioned before, and  $k$  is the rate constant. On the other hand, the zero-order kinetics based on Eq. (2) was adopted to express the photodegradation of MO using pH-9.

$$\ln\left(\frac{C_0}{C}\right) = kt \quad (1)$$

$$C = C_0 - k't \quad (2)$$

Figs. 13-14 show the pseudo-first and zero order kinetics plots for reaction of MO removal by all ZnO samples. Correlation coefficient ( $R^2$ ) were 0.98635, 0.95032, and 0.98131 for pH-7, pH-13 and pH-9, respectively. All  $R^2$  indicate that the photodegradation of MO fit well with the different kinetic models. A pseudo-first order reaction kinetics would be expected if surface reaction sites are not saturated. In this case, the kinetics follows the Langmuir–Hinshelwood law, which causes the reaction rate to be proportional to the MO concentration at low concentrations [27]. On the other hand, zero order reaction shows that the destruction of dye is independent from its concentration in the solution. This would be the case if the reaction sites on the surface are saturated and/or the reaction rate is limited by the supply of the charge carriers to the interface [28][29] [30].

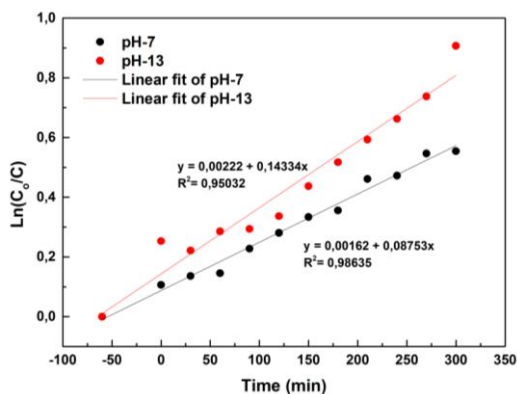


Figure 13 Pseudo first-order plots of  $\ln(C_0/C)$  versus time.

According to Kislov et al. [29], the different reaction order between the pH-7 and pH-13 (pseudo-first order) and the pH-9 (zero order),

could be related to the different polar and non-polar faces exhibited by the different samples. However, more theoretical and experimental research must be done in this direction.

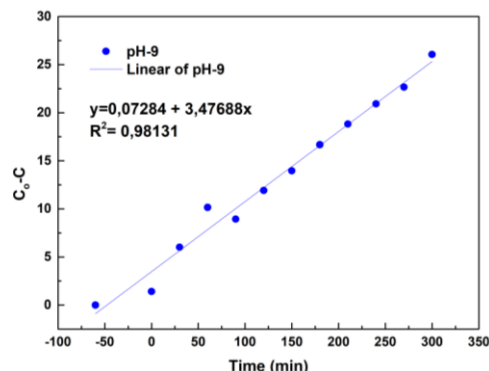


Figure 14 Zero-order plot of  $C_0-C$  versus time.

## Conclusions

ZnO nanoparticles have been prepared using the microwave-assisted method. The use of microwave heating has advantages compared with conventional methods such as, energy-saving, shorter duration of synthesis, and fewer side reactions, which makes it a simple, low-cost and green synthesis method. ZnO samples with different pH values on the zinc precursor hydrolysis were obtained. FTIR, UV-Vis, EDS and SEM characterization techniques revealed the nature and purity of the ZnO. FTIR studies showed the presence of Zn-O bond vibration and the EDS confirmed the elemental composition of all samples. Variation in band gap values with maximum band gap of 3.32 eV at pH 7 and minimum band gap of 3.15 eV at pH 13 were achieved. According to the SEM results, it is found that the size of the particles is decreases with increasing pH value. A follow-up study was conducted to evaluate the photocatalytic activity of synthesized samples using MO as model dye compound. The duration of the UV irradiation was 300 min and 93.04% degradation efficiency was achieved for pH-9 sample. Finally, this study confirmed that the role of pH has important effects on the subsequent photocatalytic performance of the material.

## Acknowledgements

The authors acknowledge the financial support by Departamento Administrativo de Ciencia, Tecnología e Innovación, Colciencias, Colombia through Convocatoria No. 727-2015.

## References

- [1] C. B. Ong, L. Y. Ng, and A. W. Mohammad, "A review of ZnO nanoparticles as solar photocatalysts: Synthesis, mechanisms and applications," *Renew. Sustain. Energy Rev.*, vol. 81, no. July 2016, pp. 536–551, 2018, doi: 10.1016/j.rser.2017.08.020.
- [2] A. Nigam and S. J. Pawar, "Synthesis and characterization of ZnO nanoparticles to optimize drug loading and release profile for drug delivery applications," in *Materials Today: Proceedings*, 2019, vol. 26, doi: 10.1016/j.matpr.2020.02.554.
- [3] E. Kusiak-Nejman *et al.*, "Size-dependent effects of ZnO nanoparticles on the photocatalytic degradation of phenol in a water solution," *Appl. Surf. Sci.*, vol. 541, no. November 2020, p. 148416, 2020, doi: 10.1016/j.apsusc.2020.148416.
- [4] J. Jiang, J. Pi, and J. Cai, "The Advancing of Zinc Oxide Nanoparticles for Biomedical Applications," *Bioinorg. Chem. Appl.*, vol. 2018, p. 18, 2018.
- [5] P. K. Mishra, H. Mishra, A. Ekielski, S. Talegaonkar, and B.

- Vaidya, "Zinc oxide nanoparticles: a promising nanomaterial for biomedical applications," *Drug Discov. Today*, vol. 22, no. 12, 2017, doi: 10.1016/j.drudis.2017.08.006.
- [6] S. Sabir, M. Arshad, and S. K. Chaudhari, "Zinc oxide nanoparticles for revolutionizing agriculture: Synthesis and applications," *Sci. World J.*, vol. 2014, 2014, doi: 10.1155/2014/925494.
- [7] O. M. El-Feky, E. A. Hassan, S. M. Fadel, and M. L. Hassan, "Use of ZnO nanoparticles for protecting oil paintings on paper support against dirt, fungal attack, and UV aging," *J. Cult. Herit.*, vol. 15, no. 2, 2014, doi: 10.1016/j.culher.2013.01.012.
- [8] K. Kamburova, N. Boshkova, N. Boshkov, and T. Radeva, "Composite coatings with polymeric modified ZnO nanoparticles and nanocontainers with inhibitor for corrosion protection of low carbon steel," *Colloids Surfaces A Physicochem. Eng. Asp.*, vol. 609, 2021, doi: 10.1016/j.colsurfa.2020.125741.
- [9] R. Shashanka, H. Esgin, V. M. Yilmaz, and Y. Caglar, "Fabrication and characterization of green synthesized ZnO nanoparticle based dye-sensitized solar cells," *J. Sci. Adv. Mater. Devices*, vol. 5, no. 2, 2020, doi: 10.1016/j.jsamd.2020.04.005.
- [10] R. Kumar, G. Kumar, and A. Umar, "Zinc oxide nanomaterials for photocatalytic degradation of methyl orange: A review," *Nanosci. Nanotechnol. Lett.*, vol. 6, no. 8, pp. 631–650, 2014, doi: 10.1166/nl.2014.1879.
- [11] M. J. Chithra, M. Sathya, and K. Pushpanathan, "Effect of pH on crystal size and photoluminescence property of zno nanoparticles prepared by chemical precipitation method," *Acta Metall. Sin. (English Lett.)*, vol. 28, no. 3, pp. 394–404, 2015, doi: 10.1007/s40195-015-0218-8.
- [12] D. Dodoo-Arhin, T. Asiedu, B. Agyei-Tuffour, E. Nyankson, D. Obada, and J. M. Mwabora, "Photocatalytic degradation of Rhodamine dyes using zinc oxide nanoparticles," *Mater. Today Proc.*, no. xxxx, 2020, doi: 10.1016/j.matpr.2020.04.597.
- [13] N. Salah *et al.*, "High-energy ball milling technique for ZnO nanoparticles as antibacterial material," *Int. J. Nanomedicine*, vol. 6, pp. 863–869, 2011, doi: 10.2147/ijn.s18267.
- [14] V. Gerbreders *et al.*, "Hydrothermal synthesis of ZnO nanostructures with controllable morphology change," *CrystEngComm*, vol. 22, no. 8, 2020, doi: 10.1039/c9ce01556f.
- [15] A. Šarić, I. Despotović, and G. Štefanić, "Solvochemical synthesis of zinc oxide nanoparticles: A combined experimental and theoretical study," *J. Mol. Struct.*, vol. 1178, 2019, doi: 10.1016/j.molstruc.2018.10.025.
- [16] J. Osuntokun, D. C. Onwudiwe, and E. E. Ebenso, "Green synthesis of ZnO nanoparticles using aqueous Brassica oleracea L. var. italica and the photocatalytic activity," *Green Chem. Lett. Rev.*, vol. 12, no. 4, pp. 444–457, 2019, doi: 10.1080/17518253.2019.1687761.
- [17] J. Wojnarowicz, T. Chudoba, and W. Lojkowski, "A Review of Microwave Synthesis of Zinc Oxide Nanomaterials: Reactants, Process Parameters and Morphologies," *Nanomaterials*, vol. 10, no. 1086, 2020, doi: 10.3390/nano10061086.
- [18] S. S. Alias, A. B. Ismail, and A. A. Mohamad, "Effect of pH on ZnO nanoparticle properties synthesized by sol-gel centrifugation," *J. Alloys Compd.*, vol. 499, no. 2, pp. 231–237, 2010, doi: 10.1016/j.jallcom.2010.03.174.
- [19] M. F. Kasim, N. Kamarulzaman, R. Rusdi, and A. A. Rahman, "Effect of pH on the Crystal Growth of ZnO Nanomaterials and Their Band gap Energies," *J. Phys. Conf. Ser.*, vol. 1083, no. 1, pp. 0–5, 2018, doi: 10.1088/1742-6596/1083/1/012043.
- [20] R. Ashraf, S. Riaz, S. S. Hussain, and S. Naseem, *Effect of pH on Properties of ZnO Nanoparticles*, vol. 2, no. 10. Elsevier Ltd., 2015.
- [21] R. A. Abdol Aziz, S. F. Abd Karim, and N. A. Rosli, "The effect of pH on zinc oxide nanoparticles characteristics synthesized from banana peel extract," *Key Eng. Mater.*, vol. 797, pp. 271–279, 2019, doi: 10.4028/www.scientific.net/KEM.797.271.
- [22] L. F. Koao, F. B. Dejene, and H. C. Swart, "Effect of pH on the properties of ZnO nanostructures prepared by chemical bath deposition method," *Proceeding SAIP*, vol. ISBN: 978-, pp. 43–48, 2015.
- [23] R. Wahab, Y. S. Kim, and H. S. Shin, "Synthesis, characterization and effect of pH variation on zinc oxide nanostructures," *Mater. Trans.*, vol. 50, no. 8, pp. 2092–2097, 2009, doi: 10.2320/matertrans.M2009099.
- [24] G. Amin, M. H. Asif, A. Zainelabdin, S. Zaman, O. Nur, and M. Willander, "Influence of pH, precursor concentration, growth time, and temperature on the morphology of ZnO nanostructures grown by the hydrothermal method," *J. Nanomater.*, vol. 2011, 2011, doi: 10.1155/2011/269692.
- [25] N. Y. Mostafa, Z. K. Heiba, and M. M. Ibrahim, "Structure and optical properties of ZnO produced from microwave hydrothermal hydrolysis of tris(ethylenediamine)zinc nitrate complex," *J. Mol. Struct.*, vol. 1079, pp. 480–485, 2015, doi: 10.1016/j.molstruc.2014.09.059.
- [26] J. Tauc, *Amorphous and Liquid Semiconductors*. London, 1974.
- [27] S.-Y. Pung, W.-P. Lee, and A. Aziz, "Kinetic Study of Organic Dye Degradation Using ZnO Particles with Different Morphologies as a Photocatalyst," *Int. J. Inorg. Chem.*, vol. 2012, pp. 1–9, 2012, doi: 10.1155/2012/608183.
- [28] C. Hu, Y. C. Chu, Y. R. Lin, H. C. Yang, and K. H. Wang, "Photocatalytic dye and Cr(VI) degradation using a metal-free polymeric g-C<sub>3</sub>N<sub>4</sub> synthesized from solvent-treated urea," *Polymers (Basel)*, vol. 11, no. 1, 2019, doi: 10.3390/polym11010182.
- [29] N. Kislov, J. Lahiri, H. Verma, D. Y. Goswami, E. Stefanakos, and M. Batzill, "Photocatalytic degradation of methyl orange over single crystalline ZnO: Orientation dependence of photoactivity and photostability of ZnO," *Langmuir*, vol. 25, no. 5, pp. 3310–3315, 2009, doi: 10.1021/la803845f.
- [30] M. A. Chamjangali and S. Boroumand, "Synthesis of flower-like Ag-ZnO nanostructure and its application in the photodegradation of methyl orange," *J. Braz. Chem. Soc.*, vol. 24, no. 8, pp. 1329–1338, 2013, doi: 10.5935/0103-5053.20130168.